Location of an α-Helix in Fragment 96–133 from Bovine Somatotropin by ^{1}H NMR Spectroscopy†

Paul R. Gooley‡ and Neil E. MacKenzie*,§

Department of Molecular Biophysics and Biochemistry, School of Medicine, Yale University, New Haven, Connecticut 06510, and Department of Pharmaceutical Sciences, University of Arizona, Tucson, Arizona 85721

Received September 4, 1987; Revised Manuscript Received December 23, 1987

ABSTRACT: By use of two-dimensional NMR techniques most of the proton resonances (>90%) are assigned for the tryptic digest fragment 96–133 of bovine somatotropin in 30% 2,2,2-trifluoroethanol-d_3/70% H_2O. Qualitative analysis of the nuclear Overhauser enhancement (NOE) data indicates that a region of α-helix spans residues 106–128, while the N- and C-terminal regions assume nonregular structures. Amide-exchange rates and comparison of two-dimensional NOE spectra indicate that the most stable piece of helix spans residues 120–125 and that this piece of helix is stable in water at 25 °C. Evidence is given to support the fact that intermolecular association of the helical segments stabilizes the helix.

Pituitary bovine growth hormone (bovine somatotropin, bSt) is a 22 000 moleular weight protein essential for growth in mammals and is responsible for a number of other physiological actions. Tryptic digestion of bSt yields a number of fragments that show measurable biological activity (Sonenberg et al., 1968; Yamasaki et al., 1975; Hubbard & Liberti, 1980). One of these fragments, AII (residues 96–133), has been extensively studied with circular dichroism, which has indicated that at pH 4 the peptide consists of 32% α-helix and 10% β-sheet that decrease to 7% and 6%, respectively, at pH 9 (Chen & Sonenberg, 1977). The helical content of AII has been found to be not only pH but also concentration and ionic strength dependent (Brems et al., 1987), indicating that interactions, inter- and/or intramolecular, are required to stabilize the helical regions. The specific locations of the helical regions are not known, although on the basis of the primary sequence of bSt, Chou–Fasman predictions find an α-helical region in the segment 111–127 and β-sheet structure in the pentapeptide 101–105. The primary structures of porcine and bovine somatotropin show a high degree of homology (>90%); therefore, we may expect their secondary and tertiary structures to be equally similar. Recently, the crystal structure of a genetically engineered variant of porcine somatotropin, methionyl porcine somatotropin, has been determined (Abdel-Meguid et al., 1987). It consists of four antiparallel α-helices arranged in a left-twisted helical bundle with helix 3 spanning residues 106–128, which differs only slightly from the above Chou–Fasman predictions.

Recently, we reported the ^{1}H nuclear magnetic resonance (NMR) assignments of a number of residues of AII in H_2O (Gooley et al., 1988). In this study nuclear Overhauser enhancement (NOE) data between backbone protons showed that the N-terminal (96–110) and the C-terminal (130–133) regions assumed nonregular structures. Long-range NOEs between the ring protons of Tyr-110 and the β-protons of Ser-100 and Phe-103 and the α-proton of Asp-107 suggested that the former region folds back on itself. No backbone NOE data could be observed for the putative helical region 110–130, and it was suggested that this region is more mobile perhaps as a result of a dynamic equilibrium between conformational states. The absence of NOE data itself is not sufficient to indicate mobility differences as other interactions such as aggregation may result in short T_2 relaxation times and, hence, an inefficient transfer of magnetization. Indeed, the concentration dependence of the helical content of AII indicated by circular dichroism studies suggests that intermolecular interactions are important. Furthermore, modeling of the putative helix shows that it is amphipathic and that its stability is a consequence of an interaction between the hydrophobic surfaces of two helices (Brems et al., 1986).

In this paper we report the solution structure of AII in a solvent mix of 30% 2,2,2-trifluoroethanol-d_3 (TFE) and 70% H_2O. TFE has been used to stabilize or induce α-helices (Nelson & Kallenbach, 1986; Clore et al., 1986), and therefore the stabilization of the putative helix of AII would assist in determining both its assignment and specific location. Furthermore, it would be of interest to see if TFE stabilizes the helix in the predicted region (111–127) or in the region described to be the helix in the porcine somatotropin (106–128).

Materials and Methods

2,2,2-Trifluoroethanol-d_3 (TFE) was obtained from Cambridge Isotope Laboratories, and ^2H_2O, ^2HCl, and NaO^2H were obtained from Merck and Co. Fragment 96–133 (AII) was obtained by partial tryptic digestion and isolated as described by Graf and Li (1974). The purity of AII was determined by the criteria of a single component by reverse-phase high-performance liquid chromatography (HPLC) (Brems et al., 1985) and polyacrylamide gel electrophoresis (Swank & Munkres, 1971).

Peptide samples were prepared by dissolving fresh peptide in either ^2H_2O or H_2O and mixing with deuteriated TFE, adjusting the pH with small amounts of dilute deuteriated or nondeuteriated HCl or NaOH as required to approximately pH 3.6, and finally adjusting the sample volume to obtain 30% TFE/70% H_2O (v/v). Reported pH values are pH meter readings uncorrected for isotope effects. The effect of TFE on pH readings was assessed by measuring the difference (0.22 pH unit) between the pH of 0.01 mM HCl with and without 30% TFE (Nelson & Kallenbach, 1986). Similarly, a cor-

† This work was supported by The Upjohn Company, Kalamazoo, MI 49001.

* Address correspondence to this author.
‡ Yale University.
§ University of Arizona.

0006-2960/88/0427-4032$01.50/0

rection of 0.10 pH unit was determined for solutions containing 15% TFE. pH readings for peptide solutions containing TFE are corrected by these differences and are indicated as pH*. To minimize the accumulation of salt and paramagnetic metal ions, peptide samples were regularly freeze-dried and chromatographed in distilled water on Sephadex G-10 columns.

^{1}H NMR spectra were recorded at 400 MHz on a Bruker AM-400 spectrometer equipped with digital-phase shifters and an Aspect 3000 computer; 5 mm outer diameter spinning sample tubes (Wilmad Glass Co., 507-PP grade) were used. Typical one-dimensional spectral acquisition parameters were as follows: spectral width 4000 Hz, 90° radio frequency pulse (5 μs), 1.0-s delay between transients, and 8096 time domain addresses. Prior to Fourier transformation the spectra were multiplied by a Lorentz–Gauss window function and zero-filled to 16 384 addresses. Chemical shifts are expressed in ppm downfield from 3-(trimethylsilyl)propionic acid (TSP) but were measured from a trace of internal dioxane at 3.748 ppm.

Two-dimensional (2D) double quantum filtered phase-sensitive homonuclear correlated spectra (DQF-COSY) were recorded by using the pulse sequence t_0–90°–t_1–90°–Δ–90°–t_2 (Rance et al., 1983), where t_1 and t_2 are the evolution and detection periods, respectively, and Δ is a 3-μs delay. The second and third 90° pulses were replaced by composite 90° pulses to reduce t_1 noise in the 2D Fourier transformed spectrum. Two-dimensional phase-sensitive nuclear Overhauser enhancement (NOESY) spectra were recorded with the pulse sequence t_0–90°–t_1–90°–τ_m–90°–t_2 (Jeener et al., 1979), where τ_m is the mixing period, usually 200 ms. To suppress contributions from coherent magnetization, the mixing time was randomly varied by ±10%. Two-dimensional homonuclear Hartman–Hahn MLEV17 spectra (HOHAHA) were recorded with the pulse sequence t_0–90°–t_1–SL_x-(MLEV17)SL_x–t_2 (Bax & Davies, 1985), where SL_x is a 2.5-ms trim pulse applied along the x axis to defocus magnetization not parallel with the x axis. The pulse widths were attenuated so that a 90° pulse was about 45 μs. The total time of the MLEV17 pulse train was 62 or 85 ms, sufficiently long to observe remote connectivities for up to five bonds ($N^\epsilon H$ to $C^\alpha H$ of Arg). All two-dimensional experiments were acquired with the time proportional incrementation scheme (Redfield & Kunz, 1975; Marion & Wüthrich, 1983). Usually 512 t_1 values were acquired for DQF-COSY and HOHAHA spectra and 448 t_1 values for NOESY spectra, and each free induction decay consisted of 2048 data points. All experiments were recorded with the spectral width of 4000 Hz in both dimensions. The water resonance was suppressed by low-power irradiation applied continuously during t_0 (usually 1.5 s) and in NOESY spectra also during τ_m.

Processing of two-dimensional spectra was performed on a MicroVAX II utilizing FT NMR (M-R Resources Inc., Ashburnham, MA). All two-dimensional spectra are presented in pure absorption and consist of 2048 × 2048 real data points. Prior to Fourier transformation in the t_2 dimension, the data were multiplied by a sine-squared bell function, phase-shifted by 22°, and zero-filled to 2048 complex data points. Before Fourier transformation in the t_1 dimension, the first row was multiplied by 0.5, and then the data wre multiplied by a sine bell function, phase-shifted by 45°, and zero-filled to 2048 complex data points.

Results

Assignment of Resonances. Specific assignments of proton resonances were obtained by the technique of sequential resonance assignment by two-dimensional NMR (Wagner et al., 1981; Billeter et al., 1982; Wüthrich, 1986). Individual amino acid spin systems were identified by DQF-COSY and HOHAHA spectroscopy. Figure 1 shows a part of a DQF-COSY spectrum where the J-connectivities for the spin systems for all three Val (Val-96, Val-102, and Val-109), all three Thr (Thr-98, Thr-105, and Thr-131), all nine AMX (Phe-97, Asn-99, Ser-100, Phe-103, Ser-106, Asp-107, Tyr-110, Asp-115, and Asp-129), one of six Leu (Leu-101), and the unique spin systems of Ala-122 and Ile-120 are indicated.

Assignment of spin systems of long-chain residues such as Leu, Glu, Met, Arg, Lys, and Pro is often hampered by weak and complex cross-peaks or lack of resolution in the spectral region where the β- and γ-protons of these residues resonate. Relayed coherence spectroscopy (RELSY) (Wagner, 1983) is useful in determining remote J-connectivities within an individual spin system and, hence, circumventing resolution problems. However, RELSY suffers from certain limitations in that the efficiency of transfer of magnetization depends on the coupling constants of the spin network and T_2 relaxation times, such that for small coupling constants and short T_2 times cross-peaks tend to be weak or absent. HOHAHA spectroscopy is an alternative to RELSY and COSY as the apparent $T_{1\rho}$ can be prolonged by up to a factor of 2, making the method attractive for molecules with short T_2 values (Bax & Davies, 1985). Figure 2 shows a part of a HOHAHA spectrum where the complete spin systems of the five Glu (Glu-111, Glu-117, Glu-118, Glu-126, and Glu-128), Met-124, and Pro-132 are indicated. Assignment of the spin systems of the two Lys residues Lys-112 and Lys-114 can be determined by direct connectivities from $C^\alpha H$ and $C^\beta H_2$ and $C^\delta H_2$ to $C^\epsilon H_2$ protons in DQF-COSY spectra and by remote connectivities from their $C^\alpha H$ to $C^\epsilon H_2$ and $C^\gamma H_2$ to $C^\epsilon H_2$ resonances in HOHAHA spectra. The $C^\epsilon H_2$ protons of Lys-112 also show a remote connectivity to a $C^\beta H$ proton (Figure 2). The three Arg $N^\epsilon H$ protons resonate near 7.2 ppm (Figure 3) and show direct connectivities to their respective $C^\delta H_2$ resonances and remote connectivities to their respective $C^\alpha H$, $C^\beta H_2$, and $C^\gamma H_2$ resonances. All three $C^\alpha H$ resonances of these Arg systems show remote connectivities to their $C^\delta H_2$ protons (Figure 2), confirming the Arg assignments.

Complete and specific assignment of the Leu systems is severely limited by resonance overlap. Twelve $C^\delta H_3$ moieties of the six Leu resonate between 0.84 and 0.96 ppm, and their $C^\gamma H$ protons resonate between 1.70 and 1.90 ppm. The only exception is the $C^\gamma H$ proton of Leu-101, which is well resolved from the $C^\gamma H$ protons of the other five Leu, thus permitting the spin system of Leu-101 to be easily assigned (Figure 1). Specific assignment of the $C^\gamma H_2$–$C^\delta H_3$ of the remaining five Leu has not been possible by either direct or remote connectivities, although a number of intraresidue NOEs indicate probable assignments.

At this stage assignments are to residue type or class of residue (for example, AMX), except for the unique spin systems of Ile-120 and Ala-122. Assignment is largely based on recognizing the coupling and chemical shift pattern characteristic of residue class or type (Wüthrich, 1986; Kessler et al., 1985). Specific assignments require techniques that discriminate between the spin systems of each residue type. Discrimination can be achieved by sequential resonance assignment, which relies on connecting individual residues to their neighbors, for example, connecting a Thr spin system to a Gly and Pro would specifically assign that Thr to Thr-131. Sequential connectivities between neighboring spin systems are obtained by through-space connectivities. The most useful through-space connectivities are the nearest-neighbor distances $C^\alpha H(i)$–$NH(i+1)$ (d_1), $NH(i)$–$NH(i+1)$ (d_2), and $C^\beta H$-

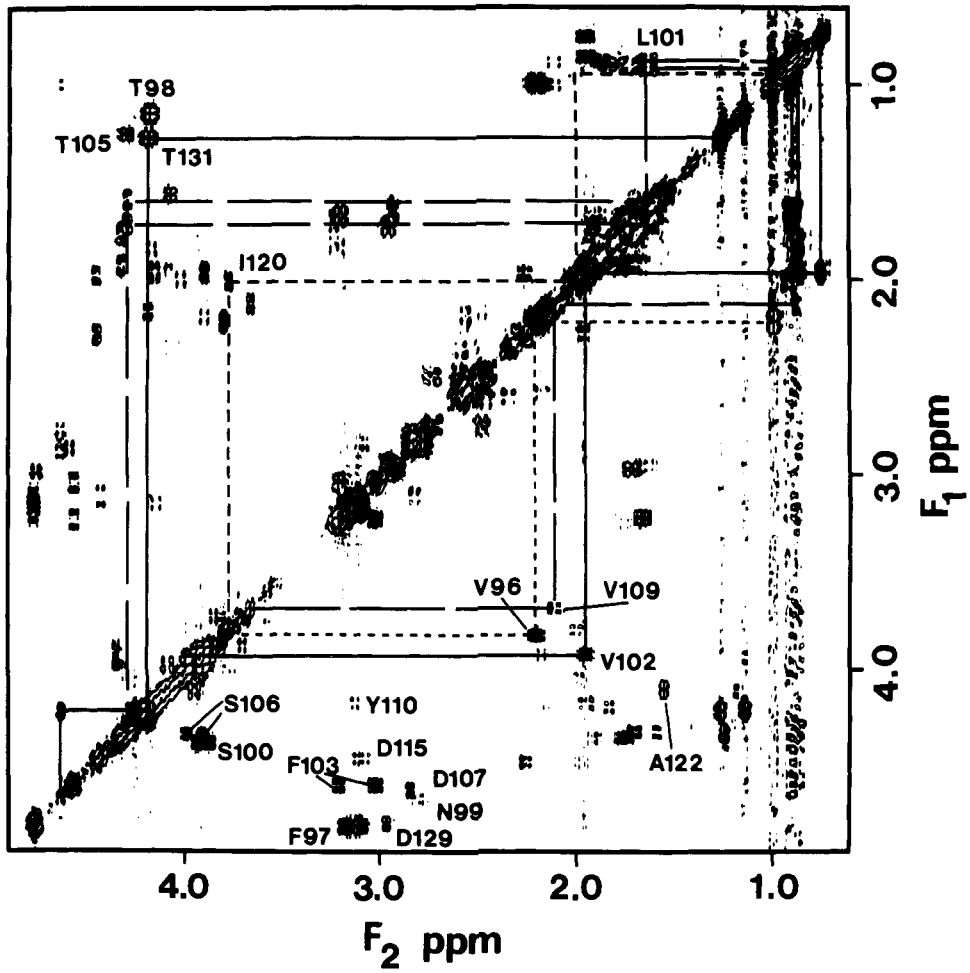

FIGURE 1: Contour plot of the spectral region F_1, F_2 = 4.92–0.62 ppm of a DQF-COSY spectrum of 8 mM AII in 30% TFE/70% ^2H_2O, pH* 3.3 at 35 °C. The J-connectivities between the $C^\alpha H$ and $C^\beta H$ protons of the nine AMX spin systems (Phe-97, Asn-99, Ser-100, Phe-103, Ser-106, Asp-107, Tyr-110, Asp-115, and Asp-129) are indicated. In addition, the complete spin systems of the three Val (Val-96, Val-102, and Val-109), Leu-101, and Thr-131 are shown. The $C^\beta H$–$C^\gamma H$ cross-peak of Thr-98 and -105 and the $C^\alpha H$–$C^\beta H$–$C^\gamma H_3$ J-connectivities of Ile-120 are also described.

(i)–NH(i + 1) (d_3). Depending on the dihedral angles, ϕ and ψ, between consecutive peptide units at least one of these distances will be less than 4 Å and will give rise to intense NOE cross-peaks for short mixing times in NOESY spectra (Billeter et al., 1982).

Prior to NOESY spectroscopy, the NH–$C^\alpha H$ J-connectivity of each amino acid spin system must be located. Figure 4 shows the spectral region of a DQF-COSY where the J-connectivities between the $C^\alpha H$ and NH resonances of AII occur. One cross-peak is expected for each residue except the N-terminus, proline, which does not have an amide proton, and glycine, which may have two cross-peaks. In Figure 4, 34 of a possible 36 cross-peaks are identified (counting only one cross-peak for each Gly residue). The spin system of Thr-131 is split into two systems, probably a consequence of cis/trans isomerism of the Thr–Pro peptide bond. The cross-peak of Glu-111 is coincident with that of Gly-130 at 35 °C but is resolved in spectra at 25 °C. The amide cross-peaks of Arg-125 and Glu-126 have not been identified, but the chemical shift of the amide resonance of each residue can be determined from NOE connectivities in NOESY spectra (see below). The chemical shift data for all proton assignments are contained in Table I.

The following paragraphs detail the evidence for the sequential assignments of AII. Figure 5 shows a part of a NOESY spectrum, recorded at 35 °C in 30% TFE/70% H_2O, where d_1 NOEs are indicated. Several short regions are sequentially assigned, 96–99, 100–103, 104–107, 108–110, 115–116, 119–120, 129–131, and 132–133. Ser-100 is connected to Asn-99 and Phe-103 to Gly-104 by d_1 NOEs in NOESY experiments recorded at 25 °C. As solvent suppression unavoidably spills over to the $C^\alpha H$ of Asn-99 and Phe-103, their connectivities are bleached from the two-dimensional spectra recorded at 35 °C. Figure 6 shows the spectral region where d_2 NOEs occur. The segment 101–106 is connected by d_2 and, as described above, d_1 NOEs. Regions that are connected by d_2 but not d_1 NOEs are 107–109, 111–113, 114–115, 116–122, 123–125, and 126–128. In addition to the d_1 and d_2 NOEs, several regions were connected by d_3 NOEs, 97–98, 101–102, 106–109, 111–112, 114–115, 120–123, 124–125, 126–127, and 129–130. NOEs beween the $C^\alpha H$ of Thr-131 and the $C^\delta H_2$ of Pro-132 are observed, thus connecting these two spin systems and indicating that the Thr-131 to Pro-132 peptide bond is predominantly in the trans configuration (Arseniev et al., 1984).

Sequential resonance assignment by d_1, d_2, and d_3 NOEs has been possible for almost the entire fragment in the solvent mix 30% TFE/70% H_2O, with breaks between Tyr-110 and Glu-111, Leu-113 and Lys-114, Ala-122 and Leu-123, and Glu-128 and Asp-129. Several of these breaks occur due to lack of resolution between amide resonances. The amide protons of Leu-113 and Lys-114 resonate at 8.19 and 8.21 ppm, respectively, and those of Glu-128 and Asp-129 at 8.12 and 8.13 ppm, respectively. The near coincidence of these pairs

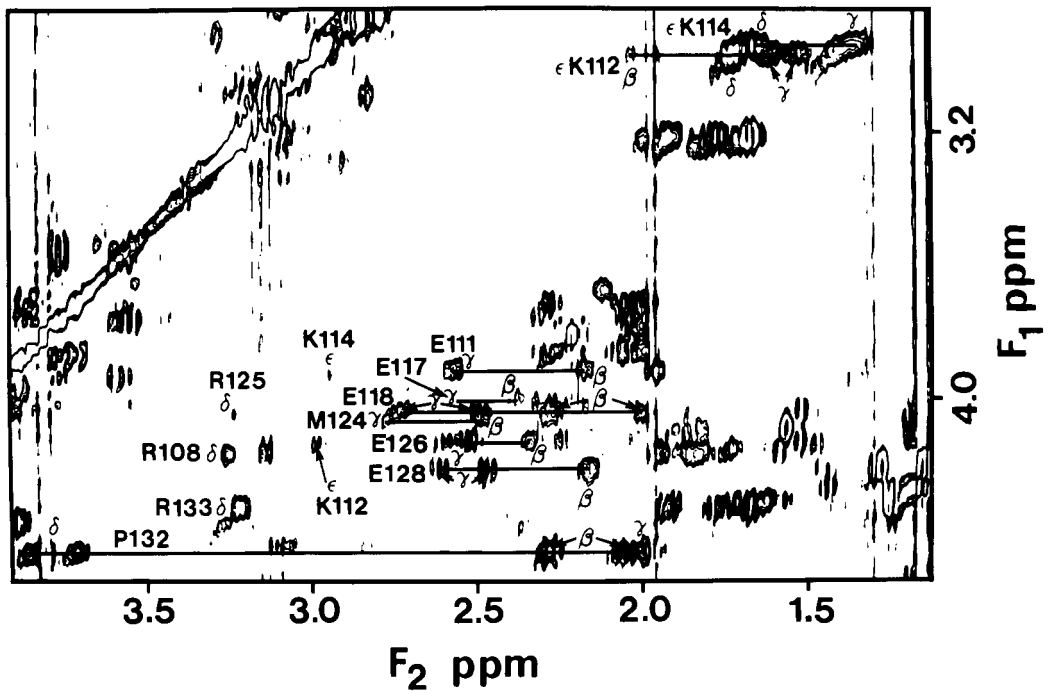

FIGURE 2: Contour plot of the spectral region F_1 = 3.92–2.84 ppm, F_2 = 4.55–1.13 ppm of a HOHAAA spectrum of 8 mM AII in 30% TFE/70% H_2O, pH* 3.3 at 35 °C, recorded with a total mixing time of 68 ms. At this mixing time both direct and remote connectivities are observed. The $C^\alpha H$–$C^\beta H$–$C^\gamma H$ connectivities for Met-124 and the five Glu (Glu-111, -117, -118, -126, and -128) and the complete spin system of Pro-132 are shown. Connectivities between the $C^\alpha H$ and $C^\delta H$ protons of Arg-108, -125, and -133 and between the $C^\alpha H$ and $C^\epsilon H$ of Lys-112 and -114 are indicated. A cross-peak between the $C^\beta H$ and $C^\epsilon H$ protons of Lys-112 distinguishes between the two Lys spin systems.

of resonances prevents connecting Leu-113 to Lys-114 and Glu-128 to Asp-129 by d_1, d_2, or d_3 NOEs. The region where the $C^\alpha H$–NH J-connectivities of Ala-122 and Leu-123 occur is very crowded. However, it is possible to connect Ala-122 to Leu-123 by a d_1 NOE in NOESY experiments where the fully protonated peptide is mixed with 30% TFE/70% ^2H_2O, and the experiment is immediately acquired. Under these conditions only amide protons that exchange slowly with the solvent deuterons give rise to a ^{1}H NMR signal.

Secondary Structure. The NOE between the peptide backbone protons of neighboring residues describes the local conformation (dihedral angles ϕ and ψ) of the peptide unit (Wüthrich et al., 1984). Elements of seconday structure can be characterized by NOE patterns observed for short mixing times and hence interproton distances of <4 Å. α-Helices are characterized by short NH(i)–NH(i + 1) distances of 2.8 Å, medium length $C^\alpha H(i)$–NH(i + 1) and $C^\alpha H(i)$–NH(i + 3) distances of 3.5 Å, and $C^\beta H(i)$–$C^\alpha H(i + 3)$ distances ranging from 2.5 to 4.4 Å. Extended chains are characterized by short $C^\alpha H(i)$–NH(i + 1) distances of 2.2 Å while all other interstrand interproton distances are >4 Å. The exception is the $C^\beta H(i)$–NH(i + 1) distance, which ranges from 3.2 to 4.0 Å for extended chains, but as this distance ranges from 2.5 to 4.0 Å for α-helix, it is not especially useful for distinguishing between these elements of secondary structure.

The NOE data between backbone protons (NH, $C^\alpha H$, and $C^\beta H$) of fragment AII in both 30% TFE/70% H_2O and H_2O are summarized in Figure 7. In TFE/H_2O the N-terminal residues 96–106 are characterized by mostly intense d_1 and medium d_2 NOEs, indicating that the conformation of this region is predominantly nonregular. The region 106–129 is characterized by medium to intense d_2, medium $C^\alpha H(i)$–$C^\beta H(i + 3)$ and $C^\alpha H(i)$–NH(i + 3), and several medium to weak d_1 and d_3 NOEs, indicating that the region 106–129 forms an α-helix in TFE/H_2O. The NOE pattern of the C-terminal segment 129–133 indicates that this segment is nonregular. In H_2O segments 96–107 and 130–133 are characterized by mostly d_1 NOEs and several d_2 NOEs. The backbone NOE pattern for these segments differs slightly from that obtained in TFE/H_2O, but there is no indication of ordered structure. However, the long-range NOEs between the ring protons of Tyr-110 and the β-protons of Ser-100 and Phe-103 and the α-proton of Asp-107, observed in NOESY spectra recorded for aqueous samples (Gooley et al., 1988), are absent in spectra recorded for 30% TFE/70% H_2O. These latter differences suggest the segment 100–110 folds back on itself in water but is more extended in 30% TFE.

Amide-Exchange Studies. Further evidence of conformation can be obtained from amide-exchange rates, which are relatively slow for amide protons participating in hydrogen bonds, and from $^3J_{HN\alpha}$ coupling constants, which are small (<5 Hz) for helices and large (>8 Hz) for extended chains. The amide region of the ^{1}H NMR spectrum of AII is very crowded, and therefore, few $^3J_{HN\alpha}$ could be resolved. After AII is dissolved in 30% TFE/70% ^2H_2O at 35 °C and pH* 3.2, most amide protons exchange readily with solvent deuterons within about 30 min, an expected time for unprotected amides (Englander et al., 1972). A number of slow-exchanging amide protons remain that have line widths of about 15 Hz, and therefore, $^3J_{HN\alpha}$ (<7.5 Hz) could not be resolved. Several of these protons, assigned to Lys-114, Glu-117, and Glu-118, exchange fully within about 200 min. The amide protons of Ile-120 and Leu-127 exchange within 400 min while those of Leu-121, Ala-122, Leu-123, and Met-124 are still present after 3000 min. Inspection of NOESY spectra recorded on AII dissolved in 30% TFE/70% ^2H_2O, but where the slow-exchanging amide protons could be observed, showed d_2 connectivities for the peptide segments 121–122 and 123–125, a d_1 connectivity between Ala-122 and Leu-123, and an NOE between $C^\alpha H$ of Ile-120 and NH of Leu-123. Thus, the amide-exchange rates and NOESY data indicate that the most stable piece of helix spans residues 120–125. Notably, there are no slow-exchanging amide proton resonances for the segments 96–110 and 129–133.

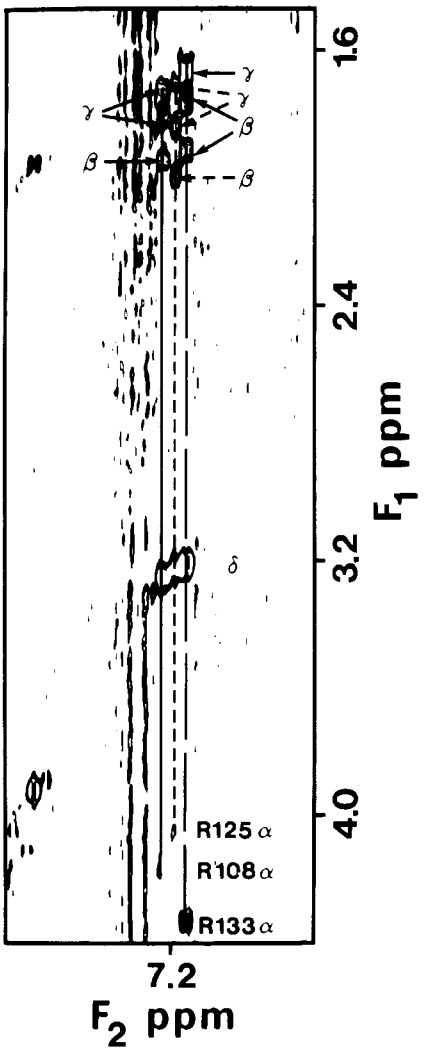

FIGURE 3: Contour plot of the same HOHAHA spectrum in Figure 2 but showing the spectral region F_1 = 4.41–1.47 ppm, F_2 = 7.73–6.75 ppm. In this spectral region, direct and remote connectivities between the $N^{\epsilon}H$ proton of the Arg residues (Arg-108, -125, and -133) and other protons of these spin systems are observed. Although the complete assignment of the Arg spin systems is possible in this experiment, care is needed in distinguishing between the $C^{\beta}H$ and $C^{\gamma}H$ protons. As these protons resonate in the same region of the spectrum, it is necessary to locate the direct coupling of the $C^{\alpha}H$ and $C^{\beta}H$ protons in either a HOHAHA experiment with small mixing times or a DQF-COSY experiment. As this direct coupling could not be observed for Arg-125, the $C^{\beta}H$ and $C^{\gamma}H$ assignments for this residue are tentative.

Amide-exchange studies on AII in ^2H_2O, 15% TFE/85% ^2H_2O, and 30% TFE/70% ^2H_2O revealed several interesting results. In all three solution conditions there are a number of slow-exchanging amides (Figure 8 and Table II). As described above, in 30% TFE/70% ^2H_2O most of these amides can be assigned to the segment spanning 120–125. Although there are significant chemical shift differences for several of these amides under the different solution conditions, we can follow the amide chemical shift dependence on TFE and therefore assign these resonances in ^2H_2O or TFE/^2H_2O mixes. NOESY spectra, recorded on protonated AII dissolved in ^2H_2O, 15% TFE/85% ^2H_2O, or 30% TFE/70% ^2H_2O but recorded in a time period where slow-exchanging amides may give rise to NOE cross-peaks, do show a number of weak d_2 cross-peaks (Figure 9), several d_3, $C^{\alpha}H(i)$–$NH(i + 3)$, and intraresidue NOEs. As the NOE patterns are qualitatively similar, in particular the medium-range NOE between $C^{\alpha}H$ of Ile-120 and the NH of Leu-123, we believe that the local α-helix conformation of the segment 120–125 is not dependent on TFE. These data are significant evidence that fragments derived from helical regions of the parent proteins can retain

Table I: Assignment of Proton Resonances of Fragment 96–133 (AII) in 30% TFE/70% H_2O, pH 3.6 at 35 °C

residue	NH	$C^{\alpha}H$	$C^{\beta}H$	others
Val-96		3.81	2.21	$C^{\gamma}H_3$ 1.02, 0.99
Phe-97	8.53	4.79	3.19, 3.11	
Thr-98	7.86	4.27	4.20	$C^{\gamma}H_3$ 1.15
Asn-99	8.08	4.65	2.86, 2.78[a]	$N^{\delta}H_2$ 7.44, 6.68
Ser-100	8.12	4.37	3.95, 3.89	
Leu-101	7.98	4.31	1.71, 1.59	$C^{\gamma}H$ 1.64; $C^{\delta}H_3$ 0.94, 0.88
Val-102	7.62	3.92	1.96	$C^{\gamma}H_3$ 0.87, 0.76
Phe-103	7.86	4.58	3.22, 3.04	
Gly-104	8.16	4.01		
Thr-105	7.94	4.28	4.32	$C^{\gamma}H_3$ 1.26
Ser-106	8.21	4.33	4.01, 3.94	
Asp-107	8.28	4.61	2.86	
Arg-108	7.96	4.16	1.95	$C^{\gamma}H_2$ 1.73, 1.82; $C^{\delta}H_2$ 3.25; $N^{\epsilon}H$ 7.22
Val-109	7.83	3.68	2.12	$C^{\gamma}H_3$ 1.01, 0.89
Tyr-110	7.89	4.17	3.13	H-3,5 7.00; H-2,6 6.82
Glu-111	8.05[b]	3.92	2.19	$C^{\gamma}H_2$ 2.57
Lys-112	7.73	4.13	2.06, 2.01	$C^{\gamma}H_2$ 1.65, 1.56; $C^{\delta}H_2$ 1.76; $C^{\epsilon}H_2$ 2.99
Leu-113	8.20	4.10	1.81	$C^{\delta}H_3$ 0.86[b]
Lys-114	8.22	3.93	1.82, 1.68	$C^{\gamma}H_2$ 1.40; $C^{\delta}H_2$ 1.70; $C^{\epsilon}H_2$ 2.96
Asp-115	8.05	4.44	3.10, 2.85	
Leu-116	8.16	4.19	1.84	
Glu-117	8.55	4.00	2.37	$C^{\gamma}H_2$ 2.61
Glu-118	8.43	4.04	1.99, 2.29	$C^{\gamma}H_2$ 2.50, 2.73
Gly-119	8.14	3.89 4.02[b]		
Ile-120	8.37	3.80	2.01	$C^{\gamma}H_3$ 0.95; $C^{\gamma}H_2$ 1.75, 1.15; $C^{\delta}H_3$ 0.83
Leu-121	8.17	4.10	1.88	
Ala-122	7.98	4.09	1.57	
Leu-123	7.93	4.16	1.84[b]	
Met-124	8.64	4.07	2.28, 2.09	$C^{\gamma}H_2$ 2.77, 2.47; $C^{\delta}H_3$ 1.97
Arg-125	8.14[b]	4.05	2.00	$C^{\gamma}H_2$ 1.71, 1.85; $C^{\delta}H_2$ 3.23; $N^{\epsilon}H$ 7.19
Glu-126	7.96[b]	4.13	2.35, 2.25	$C^{\gamma}H_2$ 2.60, 2.52
Leu-127	8.32	4.17	1.59	
Glu-128	8.13	4.21	2.18	$C^{\gamma}H_2$ 2.63, 2.47
Asp-129	8.14	4.77	2.97	
Gly-130	8.04	4.11 3.94		
Thr-131[c]	7.72	4.64	4.21	$C^{\gamma}H_3$ 1.27
Pro-132		4.46	2.28, 1.98	$C^{\gamma}H_2$ 2.05; $C^{\delta}H_2$ 3.87, 3.71
Arg-133	7.92	4.34	1.94, 1.78	$C^{\gamma}H_2$ 1.68; $C^{\delta}H_2$ 3.24; $N^{\epsilon}H$ 7.14

[a] The $C^{\alpha}H$–$C^{\beta}H$ couplings of Asn-99 are not observed at 35 °C due to solvent suppression. However, the couplings are observed at 25 °C. [b] A number of couplings could not be determined by either direct or remote methods. The chemical shifts for these resonances were determined by sequential NOEs for backbone protons or intraresidue NOEs for side chain protons. [c] Thr-131 has two spin systems as a consequence of cis/trans isomerism of the Thr–Pro peptide bond. The minor cis system is NH 7.65, $C^{\alpha}H$ 4.53, $C^{\beta}H$ 4.10, and $C^{\gamma}H_3$ 1.20 ppm.

Table II: Amide-Exchange Rate Constants ($k_m \times 10^{-3}$ min^{-1}) for Several Residues of Fragment 96–133 at 35 °C[a]

	% TFE		
residue	0	15	30
Ile-120	0.55	0.93	4.41
Leu-121	0.19	0.16	0.44
Ala-122	2.43	0.52	1.14
Leu-123	0.13	0.09	0.38
Met-124	0.36	0.20	0.57

[a] Amide-exchange rates were fitted to $\ln A = A_0 - k_m t$ (where A is measured peak intensity, A_0 is initial intensity, k_m is rate constant, and t is time). Each solution contained 8 mg of protein dissolved in 400 μL of deuteriated solvent. The pH of 0% TFE was 3.43, the pH* of 15% TFE was 3.17, and the pH* of 30% TFE was 3.20.

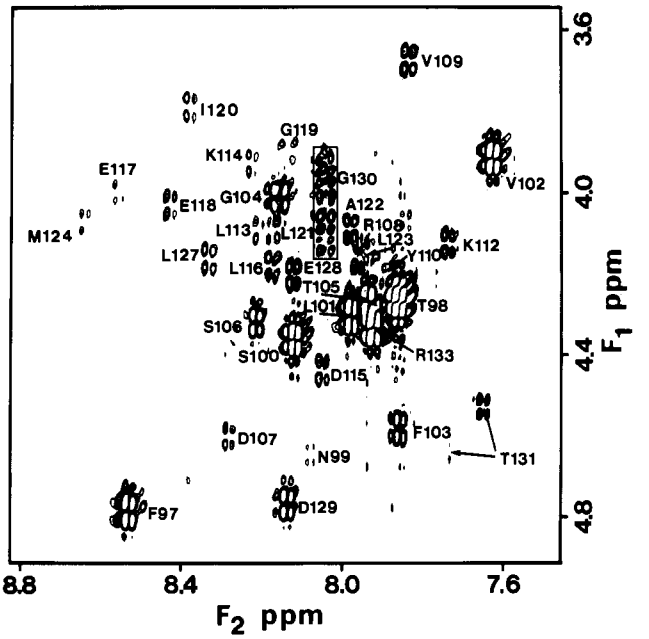

FIGURE 4: Contour plot of the spectral region F_1 = 4.92–3.55 ppm, F_2 = 8.82–7.45 ppm of a DQF-COSY spectrum of 8 mM AII in 30% TFE/70% H_2O, pH* 3.3 at 35 °C. The NH–C$^\alpha$H connectivities that have been assigned for AII are shown. The cross-peaks of Glu-111, Arg-125, and Glu-126 are missing. Under these solution conditions the connectivity for Glu-111 is coincident with Gly-130 but is resolved at 25 °C. The cross-peaks of Arg-125 and Glu-126 remain unresolved at 25 °C, but NOE connectivities indicate these resonances are near the cross-peaks of Arg-108 and Gly-119, respectively. Two cross-peaks are observed for Thr-131, most likely a consequence of cis/trans isomerism of the Thr–Pro peptide bond. The weak cross-peak at 7.72 ppm is assigned to Thr-131 of the trans isomer and the intense cross-peak at 7.65 ppm to the cis isomer. The trans isomer is the major species, but the cross-peak is weak because the C$^\alpha$H resonance of this species is coincident with the water resonance and it is unintentionally irradiated during solvent suppression. The cross-peak of Asn-99 is also weak because of spillover of irradiation during solvent suppression.

their secondary structure in aqueous solutions.

Discussion

Almost 2 decades ago, several laboratories were unsuccessful in showing that small linear peptide could form helices in aqueous solution (Epand & Scheraga, 1968; Taniuchi & Anfinsen, 1969). Short peptide are not predicted to show measurable helix formation in water according to the Zimm–Bragg equation (Zimm & Bragg, 1959) although two exceptions of peptide fragments from native globular proteins that are known to have helical structure in aqueous solution are the S- and C-peptides of ribonuclease S (Brown & Klee, 1971) and the fragment AII from bSt (Chen & Sonenberg, 1977). Zimm–Bragg calculations show that neither peptide has the theoretical potential to form a helix, and therefore other forces or interactions must contribute to the unusual stability of these fragments. Some NMR evidence has been published suggesting the location of the helical region in the S-peptide (Gallego et al., 1983; Rico et al., 1983) and that the charged group effect contributes to the stability of the helix (Shoemaker et al., 1985). The concentration and pH dependence of the helix of AII indicates that intermolecular forces may be important in stabilizing this helix, the location of which has only been predicted. To this date no NOE evidence at room temperature has been presented to show that a linear peptide has a preferred helical conformation in water. A conformation must have a sufficiently long lifetime for a proton pair to give rise to an NOE; therefore, it is important to note that any structural determinations, qualitative or quantitative, are "NOE-averaged" structures. There is published evidence that

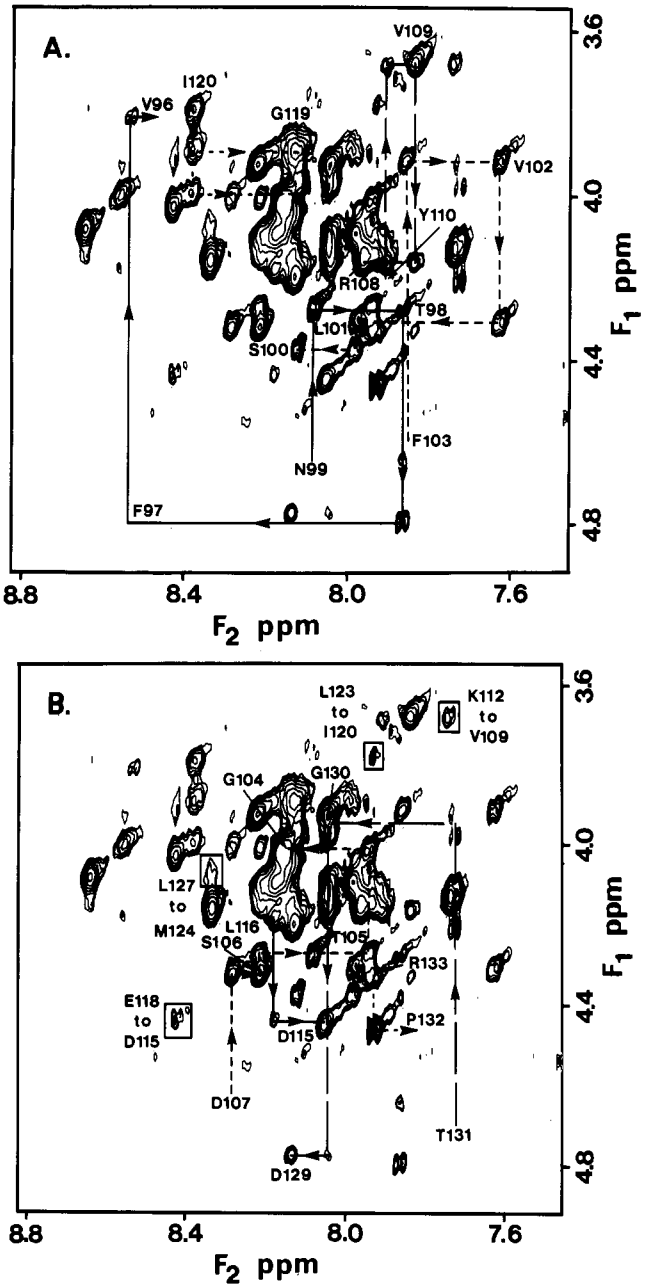

FIGURE 5: Contour plot of the spectral region F_1 = 4.92–3.55 ppm, F_2 = 8.82–7.45 ppm of a NOESY spectrum of 8 mM AII in 30% TFE/70% H_2O, pH* 3.3 at 35 °C. For clarity the same region is presented in both (A) and (B). (A) Sequential resonance assignments by C$^\alpha$H(i)–NH(i + 1) connectivities for the peptide segments Val-96 to Asn-99 (—), Ser-100 to Phe-103 (---), Arg-108 to Tyr-110 (––), and Gly-119 to Ile-120 (···) are described. (B) Sequential resonance assignments by C$^\alpha$H(i)–NH(i + 1) connectivities for the peptide segments Gly-104 to Asp-107 (---), Asp-115 to Leu-116 (—), Asp-129 to Thr-131 (––), and Pro-132 to Arg-133 (···) are described. Boxed cross-peaks are C$^\alpha$H(i)–NH(i + 3) connectivities.

linear peptides can form other preferred conformations that can give rise to NOEs; for example, a nonapeptide from haemagglutinin forms a stable reverse turn (Dyson et al., 1985). For this latter example the NMR solution structure of the peptide is not present in the X-ray crystal structure of the native protein, and it has been suggested that the nonapeptide structure may be that of a folding intermediate.

In this paper we have presented NOE evidence that an α-helix is present in the segment 106–129 in AII in 30% TFE/70% H_2O. This information in itself is not especially significant as TFE is known to induce and stabilize helices. TFE, however, may serve as a useful probe for increasing any

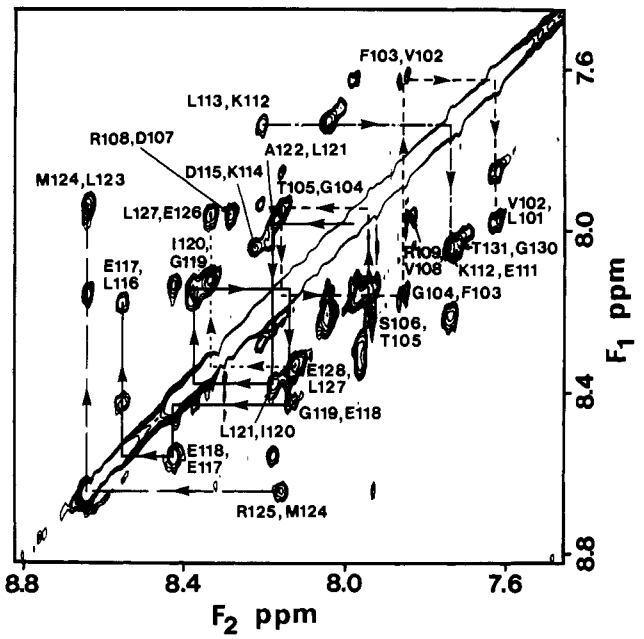

FIGURE 6: Contour plot of the spectral region F_1, F_2 = 8.82–7.45 ppm of a NOESY spectrum of 8 mM AII in 30% TFE/70% H_2O, pH* 3.3 at 35 °C. Sequential resonance assignments by NH(i)–NH(i + 1) NOE connectivities for the peptide segments Leu-101 to Ser-106 (---), Glu-111 to Leu-113 (– – –), Leu-116 to Leu-121 (—), Leu-123 to Arg-126 (– –), and Glu-126 to Glu-128 (···) are described. Also shown are NOE connectivities between Asp-107 and Arg-108, Arg-108 and Val-109, and Lys-114 and Asp-115.

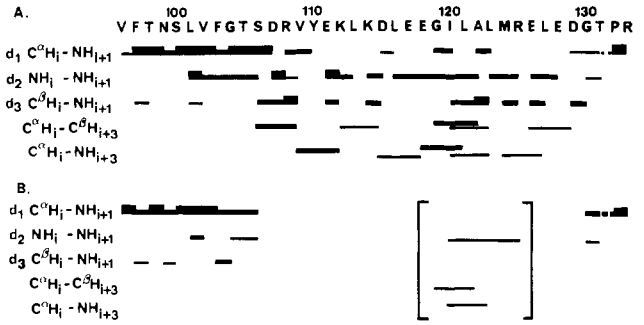

FIGURE 7: Amino acid sequence of AII and summary of NOE connectivities involving NH, $C^{\alpha}H$, and $C^{\beta}H$ protons observed in NOESY spectra for (A) 8 mM AII in 30% TFE/70% H_2O or ^2H_2O, pH* 3.3 at 35 °C, and (B) 8 mM AII in H_2O or ^2H_2O, pH 3.2 at 25 °C. The intensity of the cross-peak is indicated by the thickness of the bar. The NOEs enclosed in brackets in (B) were observed only in ^2H_2O.

marginal structural stability, if present, in linear natural peptides and protein fragments (Nelson & Kallenbach, 1986). For TFE to be considered a suitable probe it should not induce any additional helix. Comparison of the backbone NOE data for AII determined in H_2O and in 30% TFE shows that the nonregular structures for the segments 96–107 and 130–133 are not induced into helices (Figure 7). The NOE data in 30% TFE show residues 106–129 participate in an α-helix, and so we can compare the total α-helix content of AII in 30% TFE, as determined by NMR, with total α-helix content for AII in H_2O, as determined by circular dichroism. We can calculate an expected mean residue ellipticity for AII of about −20 500 from the NOE data (23 amide bonds out of 37 are in an α-helix) assuming a mean residue ellipticity of +3900 for random coil (Greenfield & Fasman, 1969) and −35 700 for α-helix (Chang et al., 1978). This figure compares favorably to −19 000 (equivalent to 25 amide bonds in a α-helix) as determined by circular dichroism (Brems et al., 1987), indicating that TFE induces little additional helix. Furthermore, the recently published crystal structure of porcine somatotropin

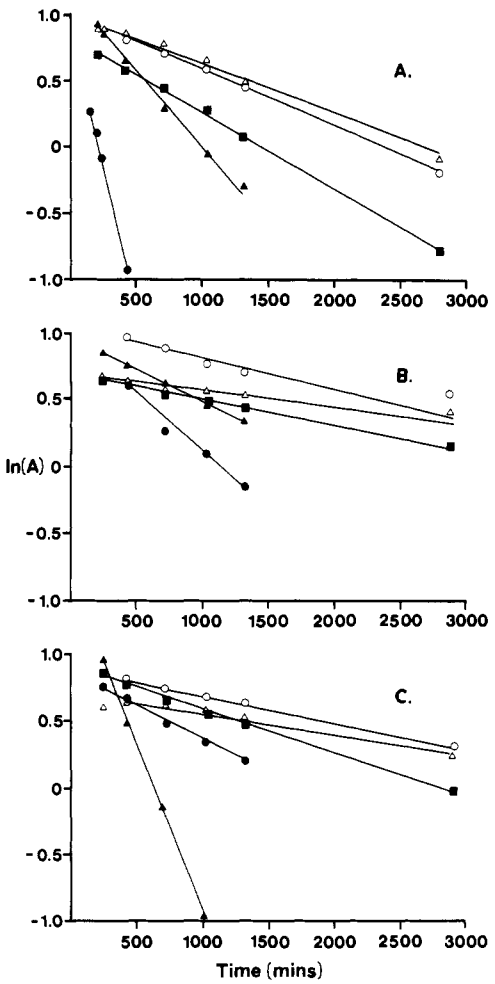

FIGURE 8: Plot of ln A (where A is the amide proton peak intensity) vs time (min) for the exchange of the amide protons of Ile-120 (●), Leu-121 (○), Ala-122 (▲), Leu-123 (△), and Met-124 (■) for solvent deuterons. The solution conditions were as follows: (A) 5 mM AII in 30% TFE/70% ^2H_2O, pH* 3.2 at 35 °C; (B) 5 mM AII in 15% TFE/85% ^2H_2O, pH* 3.2 at 35 °C; (C) 5 mM AII in ^2H_2O, pH 3.4 at 35 °C. Exchange rate constants (k_m) are in Table II.

shows an α-helix from 106 to 128, almost the same region described as α-helix by our NOE data.

The near complete assignments of AII in 30% TFE have been used to obtain more assignments in aqueous solutions where the 2D spectroscopy data is of a poorer quality. Comparison of assignment data in H_2O and TFE/H_2O and respective amide proton exchange rates shows that the most stable piece of helix encompasses residues 120–125 and is equally stable in H_2O as in mixtures of water and TFE. The dramatic difference in magnitude of the NOE response for protons in the segment 107–129 in H_2O solutions required further explanation. We believe that the postulated association of the helical region that lends stability to the helix also causes exchange broadening of many of the resonances in this region and, consequently, short T_2 times, leading to poor two-dimensional spectra. The amide resonances that are slow exchanging are markedly broader in ^2H_2O (20 Hz) than in 30% TFE/70% ^2H_2O (15 Hz), supporting a difference in T_2 times. Furthermore, weak cross-peaks may not be observed in H_2O spectra because of reduced signal to noise and t_2 stripes from the water resonance. Hydrogen bonds should show greater stability in TFE than in H_2O, but while the amide-exchange rates are slightly slower in 15% TFE than in H_2O, the rates measured in 30% TFE are consistently the fastest (Table II), suggesting that the helix is least stable in 30% TFE. The exception is the rate of exchange of the amide proton of

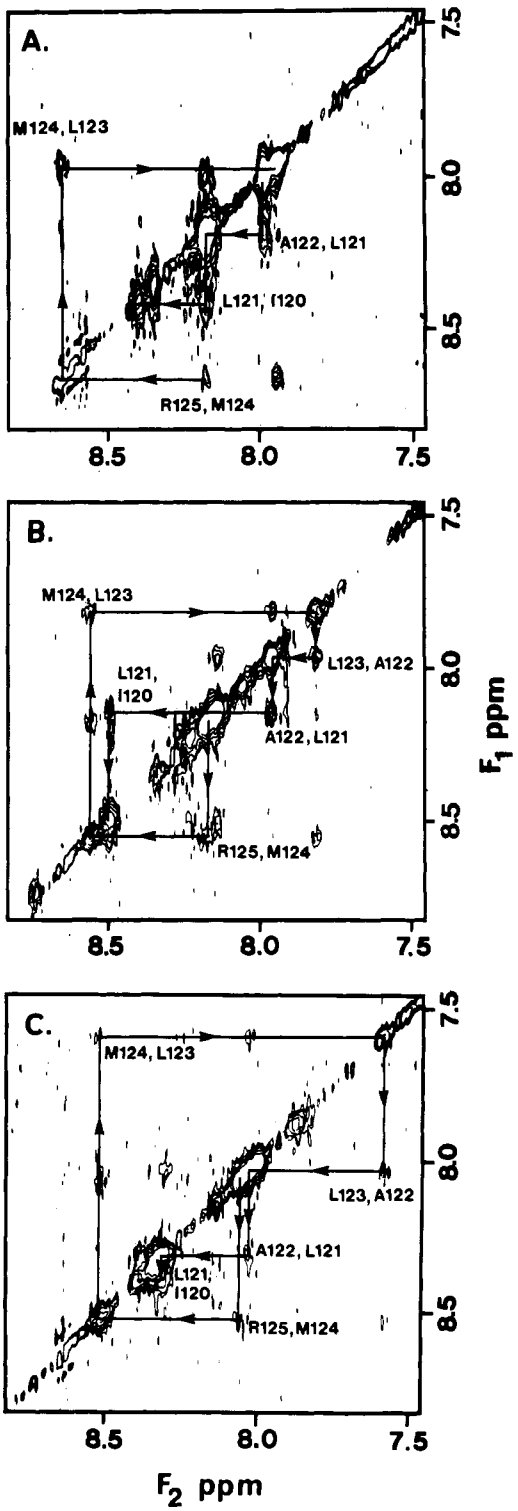

FIGURE 9: Contour plot of the spectral region F_1, F_2 = 8.82–7.45 ppm of NOESY spectra of (A) 8 mM AII in 30% TFE/70% ^2H_2O, pH* 3.3 at 35 °C, (B) 8 mM AII in 15% TFE/85% ^2H_2O, pH* 3.4 at 35 °C, and (C) 7 mM AII in ^2H_2O, pH 3.2 at 25 °C. Each sample was prepared by dissolving fully protonated AII in approximately 200 μL of ^2H_2O, adjusting the solution conditions to the above pH and TFE concentrations, and acquiring data within a 24-h period.

Ala-122, which exchanges fastest in H_2O, followed by 30% TFE and then 15% TFE. These data can be explained if both hydrogen bonding and association protect the amide protons from solvent deuterons and if TFE destabilizes association. Thus, the associated form of AII must have Ile-120, Leu-121, Leu-123, and Met-124 on the interacting hydrophobic face of the α-helix, while Ala-122 is on the noninteracting hydrophilic face, and indeed the postulated amphipathic helix has this orientation. At 0% TFE, association is the predominant helix-stabilizing force, and both hydrogen bonds and association protect amides from solvent deuterons. In 15% TFE there is a slight increase in helix stability, a consequence of the helix-stabilizing properties of TFE and the association of AII not being significantly disturbed. At 30% TFE, however, the association of AII is markedly reduced; thus the stabilizing force contributed by association is decreased and the helix is less stable than at 15% TFE. Comparing the exchange rates in ^2H_2O with those in 30% TFE, we expect faster exchange rates for the amide protons on the hydrophobic face in the latter solvent, a consequence of decreased association. The amide-exchange rate of Ala-122, situated on the hydrophilic face of the helix, is independent of the degree of association and dependent only on helix stability. As it exchanges more slowly in 30% TFE than in ^2H_2O, this exchange rate suggests that the helix is more stable in the former solvent.

The amide resonances of the segment 120–125 show varying chemical shift dependences on TFE. Ala-122, as expected, shows almost no effect, whereas Leu-123 and Met-124 show shifts to higher field with increasing TFE. These shifts may be explained as decreased association and hence solvent exposure of the amide protons. The increased shielding due to reduced hydrogen bonding from the NH to the less basic TFE would result in shifts to higher field (Nelson & Kallenbach, 1986). The amides of Ile-120, Leu-121, and Arg-125 do not show progressive trends, but Ile-120 and Leu-121 show net small shifts to higher field, and Arg-125 shows a net shift to lower field. A number of other amide protons, unassigned in H_2O, that are more slowly exchanging in ^2H_2O than in 30% TFE also show a chemical shift dependence on TFE. These amides belong to the helical region 106–129, and association is both stabilizing the hydrogen bonds and reducing solvent access to these protons.

The $C^\epsilon H_3$ protons of Met-124 resonate at 1.75 ppm in H_2O and shift toward random coil position (2.1 ppm) with the addition of TFE (1.95 ppm with 30% TFE), indicating a conformational change, but the $C^\beta H_3$ protons of Ala-122 do not shift with the addition of TFE. As Met-124 is on the interacting face of the helix and Ala-122 on the noninteracting face and as the backbone NOE pattern is similar in the various solvent mixtures for peptide segment 120–125, we suggest that the conformational difference is not a change in secondary structure but a change in extent of association. We have not observed any NOEs between the $C^\epsilon H_3$ of Met-124 and any other protons, in particular aromatic protons; thus the specific cause of this shift remains unknown.

Association of AII, therefore, appears to be a predominant force in stabilizing the α-helix region. This result supports the face that additional tertiary forces are necessary to stabilize ordered structures such as α-helices in proteins. A further example of helix-stabilizing forces is the charged group effect, a phenomenon believed to contribute to the stability of the helix in the S-peptide (Shoemaker et al., 1985). As there are a number of charged residues in AII, the charged group effect may contribute to its helix stability. However, there are a number of negatively charged residues near the C-terminus, and these charges would tend to destabilize the helix. There are several oppositely charged residues sufficiently close to interact and form salt bridges. These potential interactions may also contribute to helix formation and stability. The dissection of forces contributing to the helix stability of AII may prove difficult, although amino acid substitutions that either prevent or enhance association, the charged group effect,

or salt bridges may provide a means for studying these phenomena in AII. The association phenomenon of the α-helix of AII may not be only an in vitro artifact but could play a role in the physiological functions of the native protein, such as stabilizing folding intermediates or receptor recognition.

ACKNOWLEDGMENTS

We thank Dr. David Brems and Scott Plaisted for providing fragment 96–133, Drs. Keith Cross and Bridget Mabbut of the University of New South Wales, Australia, for providing the DQF-COSY pulse sequence with composite 90° pulses, and Judy Anet for preparing diagrams.

Registry No. Fragment 96–133, 37239-89-7.

REFERENCES

Abdel-Meguid, S. S., Sheih, H., Smith, W. W., Dayringer, H. E., Violand, B. N., & Bentle, L. A. (1987) *Proc. Natl. Acad. Sci. U.S.A. 84*, 6434–6437.

Arseniev, A. S., Kondakov, V. I., Maiorov, V. N., & Bystrov, V. F. (1984) *FEBS Lett. 165*, 57–62.

Bax, A., & Davies, D. G. (1985) *J. Magn. Reson. 65*, 355–360.

Billeter, M., Braun, W., & Wüthrich, K. (1982) *J. Mol. Biol. 155*, 321–346.

Brems, D. N., Plaisted, S. M., Havel, H. A., Kauffman, E. W., Stodola, J. D., Eaton, L. C., & White, R. D. (1985) *Biochemistry 24*, 7662–7668.

Brems, D. N., Plaisted, S. M., Kauffman, E. W., & Havel, H. A. (1986) *Biochemistry 25*, 6539–6543.

Brems, D. N., Plaisted, S. M., Kauffman, E. W., Lund, M., & Lehrman, S. R. (1987) *Biochemistry 26*, 7774–7778.

Brown, J. E., & Klee, W. A. (1971) *Biochemistry 10*, 470–476.

Chang, C. T., Wu, C.-S., & Yang, J. T. (1978) *Anal. Biochem. 91*, 13–31.

Chen, C.-J. H., & Sonenberg, M. (1977) *Biochemistry 16*, 2110–2118.

Clore, G. R., Martin, S. R., & Gronenborn, A. M. (1986) *J. Mol. Biol. 191*, 553–561.

Dyson, H. J., Cross, K. J., Houghten, R. A., Wilson, I. A., Wright, P. E., & Lerner, R. A. (1985) *Nature (London) 318*, 480–483.

Englander, S. W., Downer, N. W., & Teitelbaum, H. (1972) *Annu. Rev. Biochem. 41*, 903–924.

Epand, R. M., & Scheraga, H. A. (1968) *Biochemistry 7*, 2864–2872.

Gallego, E., Herranz, J., Nieto, J. L., Rico, M., & Santoro, J. (1983) *Int. J. Pept. Protein Res. 21*, 242–253.

Gooley, P. R., Plaisted, S. M., Brems, D. N., & MacKenzie, N. E. (1988) *Biochemistry 27*, 802–809.

Graf, L., & Li, C. H. (1974) *Biochemistry 13*, 5408–5415.

Greenfield, N., & Fasman, G. D. (1969) *Biochemistry 8*, 4108–4116.

Hubbard, J. R., & Liberti, J. P. (1980) *Biochim. Biophys. Acta 627*, 207–214.

Jeener, J., Meier, B. H., Bachmann, P., & Ernst, R. R. (1979) *J. Chem. Phys. 71*, 4546–4553.

Kessler, H., Bermel, W., Müller, A., & Pook, K. (1985) *Peptides (N.Y.) 7*, Chapter 9, 438–475.

Marion, D., & Wüthrich, K. (1983) *Biochem. Biophys. Res. Commun. 113*, 967–974.

Nelson, J. W., & Kallenbach, N. R. (1986) *Proteins 1*, 211–217.

Rance, M., Sørensen, O. W., Bodenhauser, G., Wagner, G., Ernst, R. R., & Wüthrich, K. (1983) *Biochem. Biophys. Res. Commun. 117*, 479–485.

Redfield, A. G., & Kunz, S. D. (1975) *J. Magn. Reson. 19*, 250–254.

Rico, M., Nieto, J. L., Santaro, J., Bermejo, F. J., Herranz, J., & Gallego, E. (1983) *FEBS Lett. 162*, 314–319.

Shoemaker, K. R., Kim, P. S., Brems, D. N., Marquesee, S., York, E. J., Chaiken, I. M., Stewart, J. M., & Baldwin, R. L. (1985) *Proc. Natl. Acad. Sci. U.S.A. 82*, 2349–2353.

Sonenberg, M., Kitkutani, M., Free, C. A., Nadler, A. C., & Dellacha, J. M. (1968) *Ann. N.Y. Acad. Sci. 148*, 532–558.

Swank, R. T., & Munkres, K. D. (1971) *Anal. Biochem. 39*, 462–477.

Taniuchi, H., & Anfinsen, C. B. (1969) *J. Biol. Chem. 244*, 3864–3875.

Wagner, G. (1983) *J. Magn. Reson. 55*, 151–156.

Wagner, G., Kumar, A., & Wüthrich, K. (1981) *Eur. J. Biochem. 114*, 375–384.

Wüthrich, K. (1986) *NMR of Proteins and Nucleic Acids*, Wiley, New York.

Wüthrich, K., Billeter, M., & Braun, W. (1984) *J. Mol. Biol. 180*, 715–740.

Yamasaki, N., Shimanaka, J., & Sonenberg, M. (1975) *J. Biol. Chem. 250*, 2510–2514.

Zimm, B. H., & Bragg, J. K. (1959) *J. Chem. Phys. 31*, 526–535.